Municipal Wealth and Spatial Clustering of Leprosy Incidence in São Paulo, Brazil (2017-2020): Evidence from BYM2 Modeling

Carlos Souto dos Santos Filho*
19060-900, Presidente Prudente - SP, Brazil
carlos.souto@unesp.br

Ana Júlia Alves Câmara
29.075-910, Vitória- ES, Brazil
ana.j.camara@ufes.br

Guilherme Aparecido Santos Aguilar
19060-900, Presidente Prudente - SP, Brazil
guilherme.aguilar@unesp.br

September 13, 2025

Abstract

Background: Leprosy remains a significant public health challenge in Brazil, with distinct spatial and temporal patterns reflecting underlying socioeconomic inequalities. This study investigated the association between municipal socio-territorial indicators and the geographic distribution of leprosy in São Paulo State.

Methods: A total of 4,562 new leprosy cases reported across 645 municipalities from 2017-2020 were analyzed using Bayesian spatial modeling. The Besag-York-Mollié 2 (BYM2) model was implemented to estimate relative risk while accounting for spatial dependence, incorporating municipal wealth as a covariate. Expected case counts were calculated based on overall state incidence rates and local population sizes. Exceedance probabilities were computed to identify high-risk clusters using a threshold of relative risk >2.0.

Results and Discussions: Relative risk estimates ranged from 0.06 to 31.52 (median: 0.96), with substantial spatial heterogeneity across municipalities. Municipal wealth demonstrated a significant protective effect (posterior mean: -0.059, 95% CrI: -0.081 to -0.037), indicating lower leprosy incidence in economically advantaged areas. The mixing parameter (φ = 0.517) revealed approximately equal contributions of structured spatial and unstructured random effects. High-risk clusters were predominantly concentrated in western and northern regions of the state.

Conclusions: Leprosy distribution in São Paulo State exhibits significant spatial clustering associated with municipal wealth disparities. The persistent geographic patterns suggest sustained socioeconomic determinants affecting disease transmission. These findings support targeted public health interventions in identified high-risk areas and emphasize the importance of addressing structural inequalities in leprosy control strategies.

Keywords: leprosy, spatial statistics, disease mapping, Bayesian inference, socioeconomic factors.

Background

Hansen's disease, caused by *Mycobacterium leprae* and *Mycobacterium lepromatosis*, is a chronic infectious disease ranking as the second most common mycobacterial infection worldwide after tuberculosis (Grijsen et al., 2024). The bacteria target Schwann cells and dermal macrophages, causing peripheral neuropathy, cutaneous manifestations, and mucosal lesions that may progress to motor and sensory impairments, deformities, and stigmatizing wounds. In addition to its clinical impact, historically, the disease carries profound social implications due to historical discrimination and exclusion.

Key scientific milestones include Hansen's discovery of *M. leprae* in 1874, Shepard's successful bacterial cultivation in mouse footpads at the Centers for Disease Control in 1959, and Kirchheimer and Storrs' development of the nine-banded armadillo model in 1968, which enabled disseminated infection studies. These advances significantly enhanced understanding of the disease's pathogenesis and treatment approaches (Santacroce, Del Prete, Charitos, & Bottalico, 2021).

Despite decades of public health initiatives, leprosy continues to affect populations disproportionately in low- and middle-income countries (LMICs), where poverty, poor housing conditions, and limited access to health care persist. Globally, from 1990 to 2021, the age-standardized incidence rate (ASIR) for leprosy declined by 64.79%, reaching 0.58 per 100,000 population in 2021 (Chen et al., 2024). The global burden, as measured by disability-adjusted life years (DALYs), also followed a downward trajectory, yet leprosy remains endemic in more than 120 countries. Notably, Brazil, India, and Indonesia together account for approximately 79.3% of new annual cases, with the disease particularly concentrated in tropical and subtropical regions (Grijsen et al., 2024). In these contexts, the persistence of leprosy reflects not only biological transmission mechanisms but also structural and societal inequities that facilitate the disease's spread and hinder timely diagnosis and treatment.

In Brazil, leprosy continues to represent a complex public health issue, with distinct spatial and temporal patterns. Recent investigations have documented heterogeneous relapse rates and disease clustering across the national territory. Boigny et al. (2024), using space–time scan statistics, identified high-risk clusters of leprosy relapse in the North, Northeast, and Central-West regions, characterized by relative risks (RR) ranging from 1.78 to 3.97. These clusters were frequently found in socioeconomically disadvantaged municipalities with barriers to health service access. According to the authors, these patterns are associated with both structural vulnerabilities and higher baseline infection rates, which contribute to continued transmission and recurrence of the disease.

In a complementary analysis, Sczmanski et al. (2025) assessed clinical and epidemiological data from 215,155 newly reported leprosy cases between 2014 and 2019. Their findings revealed that the disease remains stable in most Brazilian regions, with the highest detection rates in the Midwest and lowest in the South. The most affected individuals were predominantly male, literate, and of black or brown ethnicity, aged between 60 and 79 years. Multibacillary forms and borderline clinical presentations predominated, suggesting late detection and heightened transmission potential. The study emphasized that leprosy persists as a public health concern, closely linked to social inequalities and requiring spatially informed public health responses.

For a long time, the importance of epidemiology related to leprosy was neglected in spatial studies. Guided by these findings, the present study adopts a spatial epidemiology approach to investigate the association between municipal-level socio-territorial indicators and the geographic distribution of leprosy in the state of São Paulo from 2017 to 2020. By incorporating spatial statistical modeling and disease mapping techniques, this analysis aims to uncover hidden patterns of risk and support the strategic allocation of public health resources in line with the WHO's "Towards Zero Leprosy" roadmap.

The main objective of this study was to evaluate the association between municipality-level socio-territorial indicators—namely wealth, longevity, and education—and the spatial distribution of leprosy cases in the State of São Paulo from 2017 to 2020. Additionally, the study aimed to identify clusters of municipalities where the incidence of leprosy was significantly higher than expected based on available covariates, suggesting the presence of underlying social or environmental determinants not captured by standard indicators. Furthermore, the study sought to compare patterns of leprosy incidence across pre-defined socio-territorial groups of municipalities, with a particular focus on assessing whether combinations of low wealth were consistently associated with increased leprosy risk.

Methods

Study Area: State of São Paulo

Demographic data from the 2022 Brazilian Census indicate that the state of São Paulo reached a total population of 44.4 million, reflecting an increase of 3.2 million residents over the previous twelve years, corresponding to an average annual growth of 263,200 individuals. Since 1940, the population has expanded by a factor of 6.2 (IBGE, 2023). However, recent decades have witnessed a deceleration in growth rates due to declining fertility and a reduction in net migration.

Between 2010 and 2022, the capital's annual growth rate was 0.15%, significantly lower than the rates observed in the interior (0.79%) and the state as a whole (0.62%). The most recent census confirmed a reduction in the state's overall population growth rate, which fell from 1.09% in the 2000–2010 period to 0.62% in the subsequent intercensal period. This shift was accompanied by a rise in the number of municipalities experiencing population decline, increasing from 102 to 197, while the number of municipalities with positive growth declined from 543 to 448 (IBGE, 2023).

In addition to demographic indicators, the São Paulo Index of Social Responsibility (IPRS), which evaluates municipalities based on wealth, longevity, and educational attainment, revealed notable changes between 2014 and 2018. The number of municipalities classified as vulnerable, characterized by low levels in all three dimensions, decreased from 77 to 61, with a corresponding reduction in the affected population from 2.35 million (5.5%) to 2.02 million (4.6%) (Fundação SEADE, 2019). The number of dynamic municipalities, defined by their economic vitality and medium to high performance in education and longevity indicators, increased from 104 to 112, expanding the share of the population in this category from 32.1% (13.7 million) to 34.0% (15 million). Although the number of unequal municipalities, which generate wealth but exhibit low performance in either education or longevity, rose from 71 to 75, the associated population declined slightly from 45.3% (19.33 million) to 43.6% (19.18 million). Lastly, the group of equitable municipalities, which present low levels of wealth

but relatively favorable outcomes in education and longevity, increased from 212 to 218 municipalities, encompassing 9.8% (4.31 million) of the state's population in 2018, compared to 9.7% (4.14 million) in 2014 (Fundação SEADE, 2019).

Data Extraction

The health and socioeconomic information used in this study was obtained from digitized and anonymized data provided by official state agencies. The dependent variable (DV) corresponds to the number of incident cases of leprosy reported in the state of São Paulo during the period from 2017 to 2020. These data were obtained from the Technical Division of Epidemiological Surveillance of Leprosy, part of the Center for Epidemiological Surveillance of the São Paulo State Health Department.

The independent variables include socioeconomic indicators derived from the São Paulo IPRS, which encompasses municipal-level measures of wealth, longevity, and education. These indicators were obtained from the State Data Analysis System (SEADE Foundation), an agency under the Government of the State of São Paulo. All IPRS data refer to the year 2018 and are publicly available for the state's 645 municipalities.

Covariate Selection: Municipal Wealth Indicator

Among the variables considered in the statistical modeling, the municipal wealth indicator (2018), derived from the IPRS, was selected as a covariate in the Poisson regression model. The choice of this variable was based on both theoretical relevance and empirical significance.

The wealth indicator captures the economic profile of each municipality by integrating multiple components. These include electricity consumption in agriculture, commerce, and services; per capita value added; residential electricity consumption; and the average income of formally employed individuals in both the private and public sectors. These data are sourced from administrative records provided by the State Secretariats of Finance and Energy of São Paulo, as well as the Ministry of Labor and Employment. The indicator is scaled from 0 to 100 and can be reproduced annually, ensuring its applicability in longitudinal studies.

In the Poisson regression model, Wealth (2018) demonstrated a statistically significant and inverse association with the outcome variable (Estimate = -0.03878; $p < 0.001$). This finding suggests that municipalities with higher levels of economic wealth tend to present lower expected counts of incident leprosy cases. This relationship is consistent with prior literature linking socioeconomic development to improved public health and environmental outcomes, reinforcing the theoretical justification for its inclusion in the model. The other covariates, longevity and education, were also evaluated; however, only education showed a statistically significant positive association in the model (Estimate = 0.03811; $p < 0.001$), while longevity was not statistically significant ($p = 0.83$). These results inform the understanding of how multidimensional socioeconomic factors influence the phenomenon under study.

Spatial modelling: BYM2 Model

In this study, we applied the BYM2 model to estimate the spatial distribution of leprosy incidence across municipalities in the state of São Paulo. Although standardized incidence ratios (SIRs) are commonly used in spatial epidemiology, they can be unstable and misleading, particularly in areas with small populations or where the disease is rare.

In such cases, the expected number of cases may be very low, leading to high variance and potential misinterpretation of risk patterns. To address this limitation, hierarchical Bayesian models such as the BYM2 offer a more robust alternative by borrowing information from neighboring regions and integrating relevant covariates. This enables the smoothing of extreme values and enhances the stability of risk estimates (Gelfand et al., 2010; Lawson, 2009).

The BYM2 model is an updated and reparameterized version of the traditional Besag-York-Mollié (BYM) model, as proposed by Simpson et al. (2017). It enables the specification of interpretable and computationally efficient penalized complexity (PC) priors. In this model, the relative risk for area iii, denoted as λi, is modeled as:

$$Y_i \sim \text{Poisson}(E_i\lambda_i), \log(\lambda_i) = \mu + X_i\beta + U_i$$
$$U_i = W_i + V_i$$

where E_i is the expected number of cases in area $i, X_i\beta$ represents the fixed effects of covariates (e.g., municipal wealth), and U_i is a spatially structured random effect combining W_i, an intrinsic conditional autoregressive (CAR) term, and V_i, an unstructured independent noise term. In the BYM2 formulation, these components are scaled and combined into a single expression to balance structured and unstructured effects via a mixing parameter ϕ, as follows:

$$\mathbf{b} = \frac{1}{\sqrt{\tau_b}}\left(\sqrt{1-\phi}\,\mathbf{v}_* + \sqrt{\phi}\,\mathbf{u}_*\right),$$

where τ_b is the overall precision (inverse variance) of the combined spatial effect, and $\phi \in [0,1]$ controls the proportion of total variance attributed to the structured spatial component $\mathbf{u}_*$. When $\phi = 1$, the model behaves as a fully structured spatial model, whereas $\phi = 0$ corresponds to a model driven entirely by unstructured noise.

This reparameterization simplifies model interpretation and facilitates prior specification in the Bayesian framework. In particular, PC priors can be applied to penalize model complexity, thereby shrinking the structured spatial component toward a base model of no spatial variation, unless the data strongly support it. The model was implemented using the INLA (Integrated Nested Laplace Approximation) approach in R-INLA. The use of the BYM2 model in this context ensures statistically stable and spatially coherent estimates of leprosy risk, accommodating the heterogeneity in population size and enabling robust inference across small areas.

The marginal precision of the spatially structured random effect (τ_b) was assigned a penalized complexity (PC) prior defined as $P\left(\left(\frac{1}{\sqrt{\tau_b}}\right) > U\right) = a$. Following the rule of thumb by Simpson et al. (2017), a marginal standard deviation of approximately 0.5 was assumed as a reasonable upper bound and thus set $U = 0.5 / 0.31$ and $a = 0.01$, yielding the prior $P\left(\left(\frac{1}{\sqrt{\tau_b}}\right) > 1.61\right) > 0.01$. For the mixing parameter φ, which balances spatially structured and unstructured effects, we specified the prior $P(\varphi < 0.5) = 2/3$ reflecting a conservative assumption that the unstructured component accounts for more of the variability. Given the presence of 191 zeros in the dataset, we also investigated the potential for zero inflation and selected model configurations accordingly to improve computational efficiency. The final model was specified as follows:

$$\text{NewCases}_{2017-2020} \sim \beta_0 + f(\text{AreaID}, \text{model} = \text{"BYM2"}, \text{graph} = \text{Graph}, \text{hyper} = \text{Prior}) + \text{Wealth}_{2018} + \log(\text{ExpectedCases}_{2017-2020})$$

Computational Statistical Analysis

Exploratory data analysis was initially performed to detect outliers, missing values, and assess zero inflation in the response variable. A spatial neighborhood map was constructed to identify adjacent municipalities within São Paulo State, defining the neighborhood structure required for spatial modeling (Figure 1). This adjacency matrix was built using geographic boundary data to determine which municipalities share common borders, establishing the spatial relationships necessary for incorporating spatial dependence in the analysis. One isolated polygon was identified during this process. Spatial neighborhood structures were then defined based on this adjacency information to support spatial modeling, and expected counts were computed for each area i using the formula $E_i = r(s) \times n(i)$, where r(s) is the overall disease rate (total number of cases divided by the total population across all areas), and n(i) is the population of area i.

These expected counts were used to calculate the standardized incidence ratio (SIR) for preliminary spatial risk assessment. Based on exploratory patterns and covariate distributions, final model covariates were selected. The statistical analysis was conducted using R version 4.4.0, with the support of the following packages: *terra, geodata, geostatsp, mapmisc, diseasemapping, INLA*, and *tmap*.

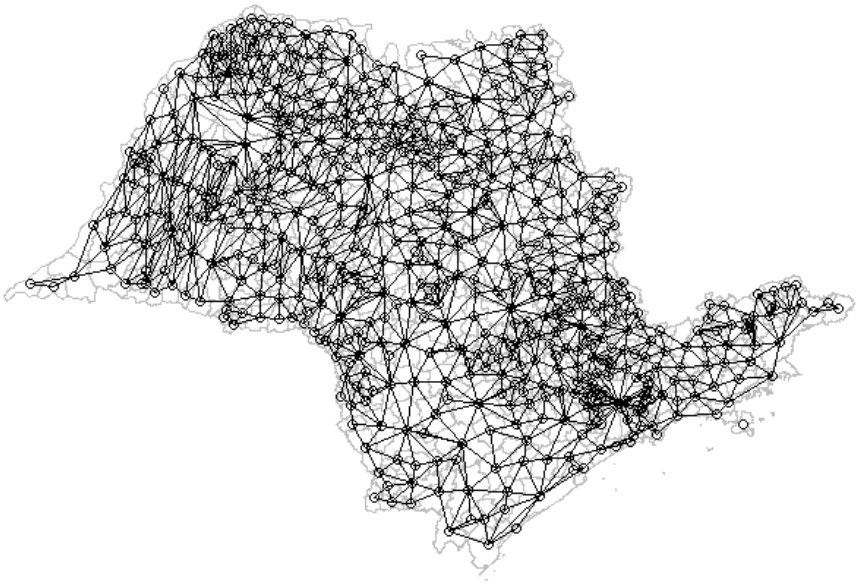

Figure 1. Neighbors of municipalities of São Paulo State.

Results and Discussions

From 2017 to 2020, a total of 4562 new leprosy cases were recorded across municipalities in the State of São Paulo, resulting in a mean of approximately 7.07 cases per municipality over the period. The number of cases ranged from 0 to 461, with a median of 2. The first quartile (Q1) was 0, and the third quartile (Q3) was 5, reflecting the presence of many municipalities with few or no recorded cases and a right-skewed distribution. Expected case counts showed a similar mean of 7.07 but had a much wider range—from 0.084 to 1,220.76—highlighting substantial heterogeneity in population size

across municipalities. The SIR ranged from 0.00 to 32.81, with a median value of 0.82 and a mean of 1.72, indicating that while most municipalities had incidence rates near or below the expected level, a subset exhibited considerably elevated risk. Socio-territorial conditions, represented by the wealth index for 2018, showed a median of 34 and a mean of 34.58, ranging from 15 to 62, suggesting moderate socioeconomic variation among municipalities.

For initial visualization of the spatial distribution of the leprosy burden in the State of São Paulo, thematic maps were constructed to represent the observed incident cases, expected cases, and SIRs for the period 2017–2020. The expected number of cases in each municipality was calculated based on the overall leprosy rate in the state and the local population size, allowing for comparisons that account for population differences. By integrating the epidemiological data with spatial boundaries at the municipal level, three distinct maps were produced to highlight different aspects of disease distribution.

These three objects are plotted in Figure 2. Although SIRs can be useful for preliminary spatial assessment, in regions with small populations or rare diseases, the expected counts may be very low. In such cases, SIRs can be unstable and insufficiently reliable for robust inference or public health reporting.

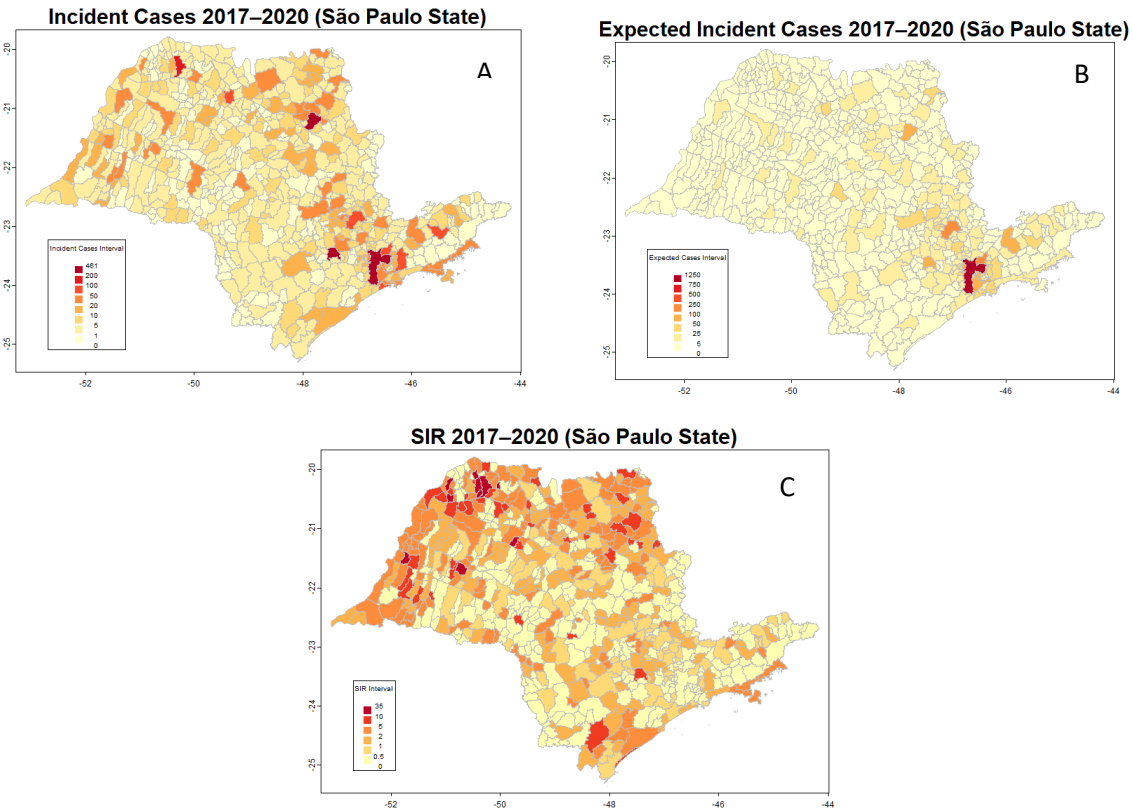

Figure 2. Spatial Distribution of Observed Cases (A), Expected Cases (B), and SIRs (C) for Leprosy (2017–2020) in São Paulo State.

Table 1 presents posterior means and 95% credible intervals for parameters from the spatial BYM2 model fitted to São Paulo leprosy data (2017-2020). The intercept was 1.138 (95% CrI: 0.362 to 1.915), indicating baseline log-risk across municipalities. Municipal wealth was negatively associated with leprosy incidence (-0.059, 95% CrI: -0.081 to -0.037), suggesting wealthier municipalities had lower relative risk after accounting for spatial structure. The precision parameter (τ) was 0.430 (95% CrI: 0.350

to 0.522), indicating moderate spatial smoothing. The mixing parameter (φ) was 0.517 (95% CrI: 0.349 to 0.684), reflecting approximately equal contributions of structured and unstructured spatial effects. The model highlights significant spatial heterogeneity in leprosy risk, with wealth as an important protective factor.

	Mean	0.025 quantile	0.975 quantile
Intercept	1.138	0.362	1.915
Wealth	-0.059	-0.081	-0.037
Precision (τ)	0.430	0.350	0.522
Phi (φ)	0.517	0.349	0.684

Table 1: Posterior means and 95% credible intervals for model parameters obtained from fitting the São Paulo leprosy data with the BYM2 model.

The posterior distribution of the wealth coefficient was plotted using smoothed marginal distributions (Figure 3).

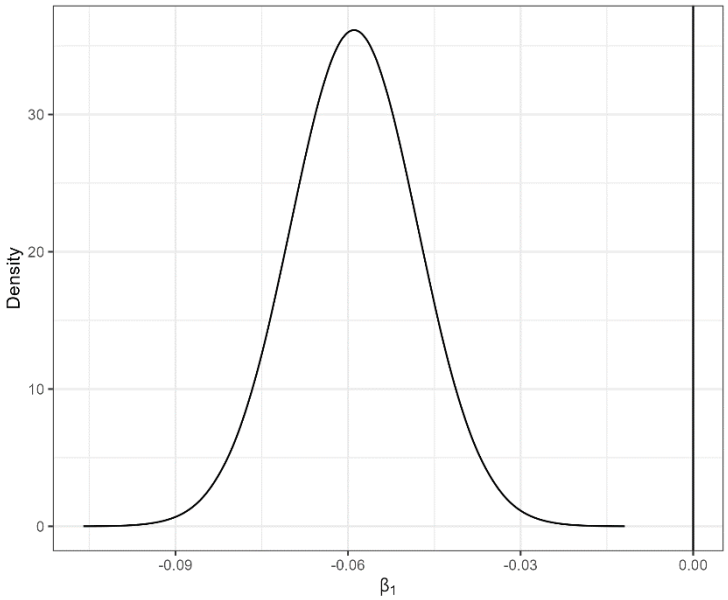

Figure 3. Posterior distribution of the coefficient of covariate wealth.

As summarized in Table 2, the relative risk (RR) of leprosy incidence derived from the spatial model ranged from 0.06 to 31.52, with a median of 0.96 and a mean of 1.75. The lower limit (LL) of the 95% credible interval varied from 0.0009 to 21.92, while the upper limit (UL) ranged from 0.35 to 53.10 (Figure 4). These values indicate that although the majority of municipalities had low or average risk, there were high-risk clusters with substantially elevated relative risk, suggesting spatial heterogeneity in the distribution of leprosy that may be associated with underlying socio-environmental determinants.

Statistic	RR	LL	UL
Min.	0.06095	0.000872	0.3514
1st Qu.	0.46445	0.048239	1.5544
Median	0.96117	0.217093	2.9310
Mean	1.74752	0.648540	4.5265
3rd Qu.	1.94335	0.568785	5.8618
Max.	31.51820	21.916249	53.0994

Table 2. Summary Statistics for RR, LL, and UL Variables.

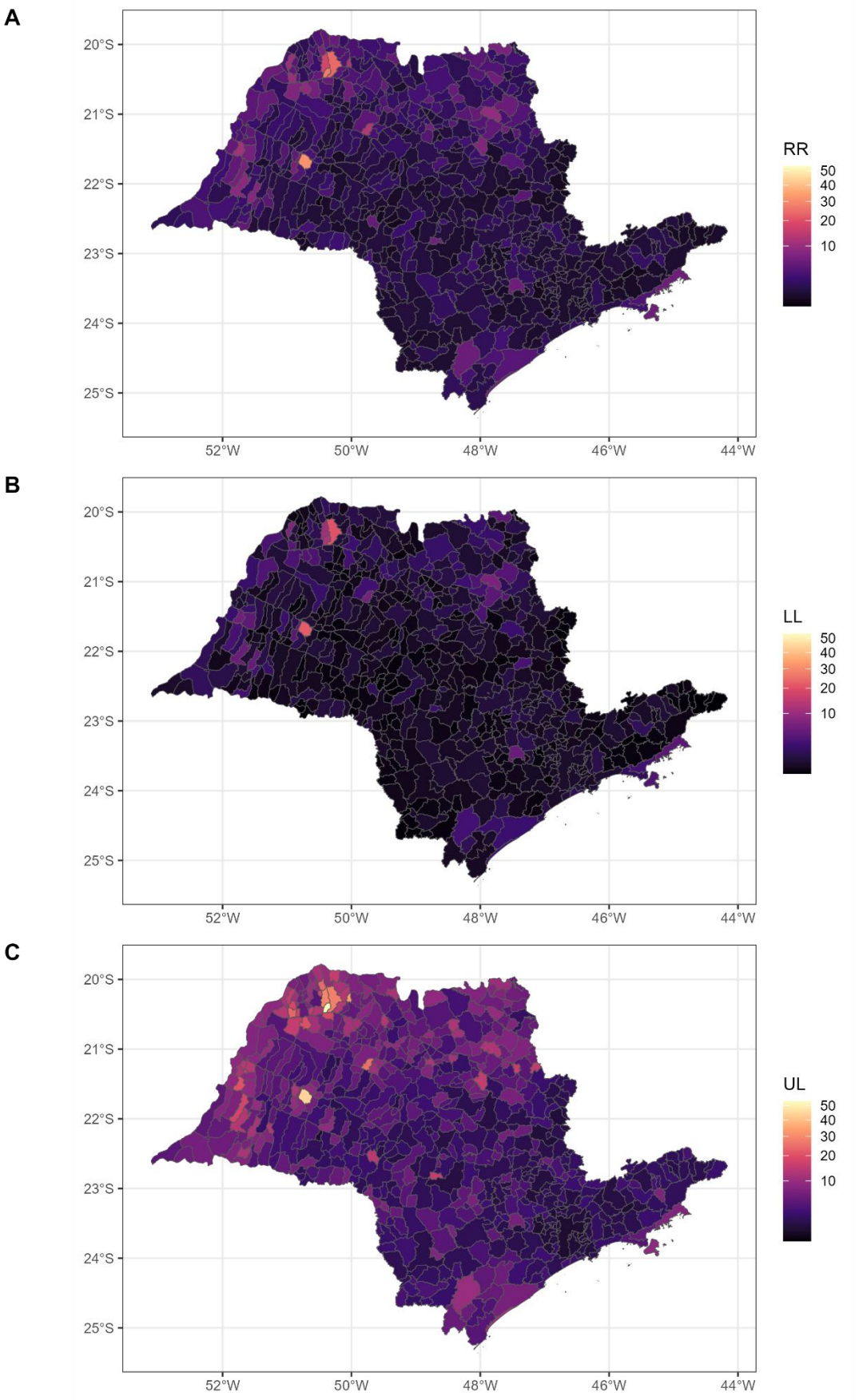

Figure 4. Mean (A) and lower (B) and upper (C) limits of 95% credible intervals of leprosy RR in São Paulo municipalities.

To further understand the spatial heterogeneity of leprosy risk beyond observed covariates, we examined the posterior mean of the spatial random effect *b* from the BYM2 model. This parameter captures unmeasured spatial variation by combining both structured (spatially correlated) and unstructured (random noise) components. Figure 5 presents the posterior mean estimates of *b* across all municipalities in São Paulo State. Positive values of *b* indicate areas with higher-than-expected leprosy risk not explained by the included covariate (wealth), while negative values suggest reduced risk or potential underreporting. This spatial residual helps identify hidden patterns of disease transmission and suggests municipalities where additional epidemiological investigation may be warranted. Mapping these latent effects provides a more nuanced understanding of disease dynamics and supports targeted public health planning beyond what is revealed by observed data alone.

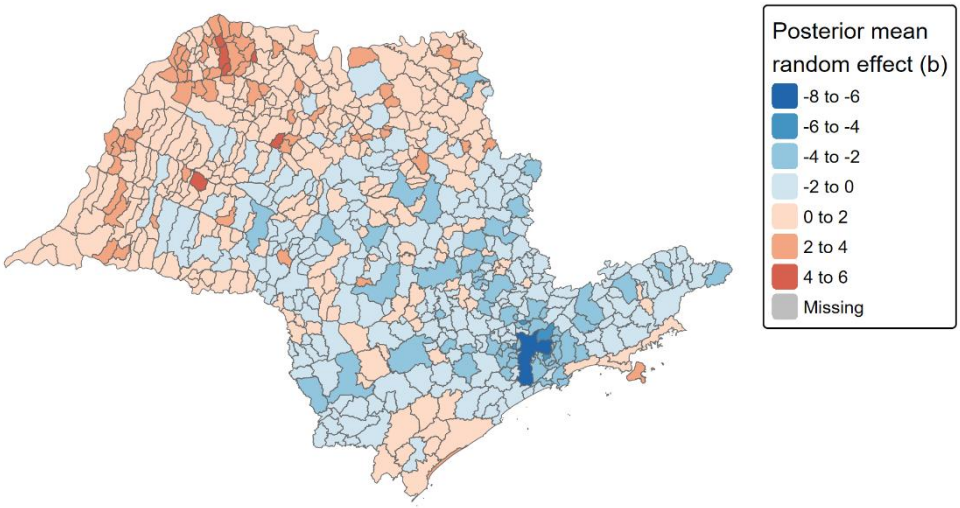

Figure 5. Posterior mean of the BYM2 random effect *b*.

To identify areas with significantly elevated leprosy risk, exceedance probabilities were calculated using a threshold of RR > 2, a criterion commonly adopted in public health to flag high-priority regions. This threshold reflects municipalities where the relative risk is at least double the state average, indicating potential hotspots of concern.

Figure 6 displays the spatial distribution of exceedance probabilities across São Paulo municipalities. The color scale aids interpretation: light yellow areas represent low probabilities (low-risk), orange to red areas indicate moderate evidence of elevated risk, and dark red to purple areas signal high probabilities (close to 1), reflecting strong statistical evidence that RR exceeds 2.

The map reveals distinct spatial patterns. Clusters of high exceedance probabilities are concentrated in the western and northern regions of the state, while southeastern coastal areas also show some persistent high-risk zones. In contrast, central and southern interior municipalities generally display low probabilities, suggesting a lower likelihood of elevated leprosy risk.

To assess the quality of the fitted BYM2 spatial model, posterior samples and densities were extracted using INLA's internal sampling functions (n = 1000). This approach enables visualization of marginal posterior distributions and contributes to evaluating model fit beyond summary statistics (Figure 7). The

extracted densities help identify the distributional behavior of key parameters and verify whether the posterior estimates are consistent with prior assumptions and data structure.

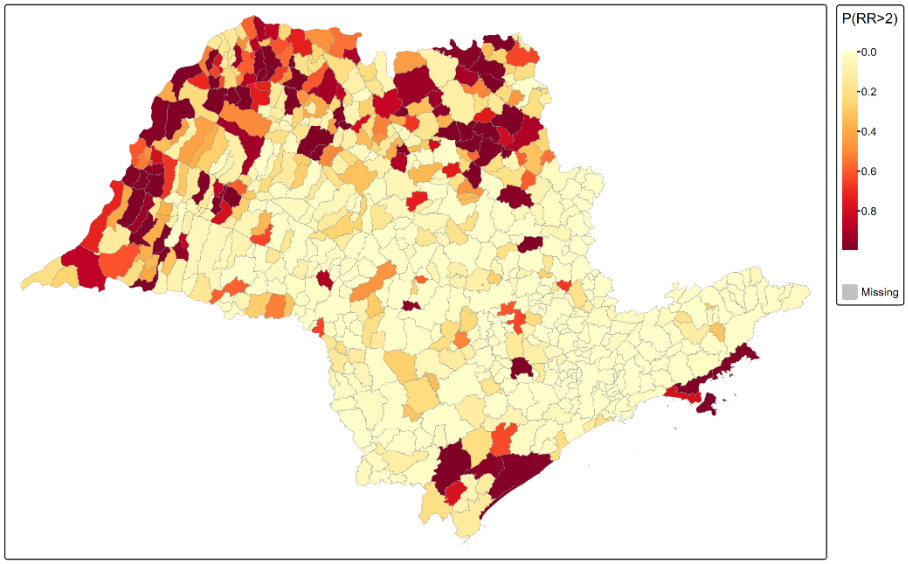

Figure 6. Exceedance probabilities for leprosy relative risk greater than 2 across municipalities in São Paulo (2017–2020).

Model fit was further assessed using the Deviance Information Criterion (DIC). The DIC value of 2526.27 reflects the balance between model fit and complexity; although not interpretable in isolation, it serves as a basis for model comparison. The Conditional Predictive Ordinate (CPO) values were also examined to evaluate predictive performance and potential outliers. The distribution of CPO values, where 98% (633 out of 645) of municipalities had CPO < 0.01, suggests low predictive accuracy in many areas. This pattern may indicate overdispersion, zero inflation, or deviation from the assumed Poisson structure in specific municipalities. These findings underscore the need to interpret spatial patterns with caution, particularly in locations with extreme or sparse data.

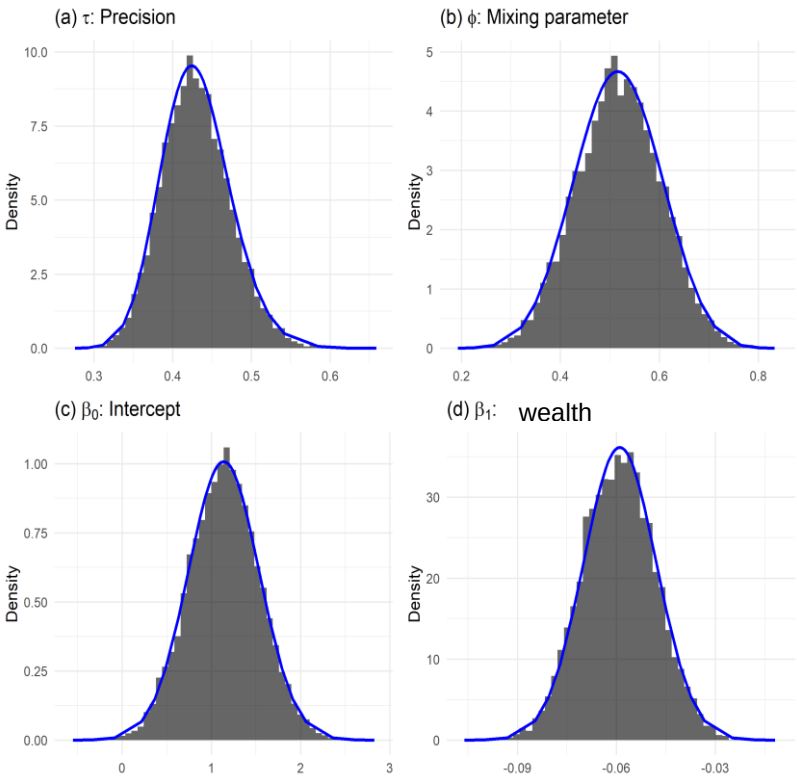

Figure 7. Histograms of posterior samples (black bars) obtained from fitting the BYM2 model using INLA (n = 1000), along with posterior densities derived from the marginal distributions (blue lines).

This study aimed to evaluate the association between municipality-level socio-territorial indicators and the spatial distribution of leprosy cases in São Paulo State from 2017 to 2020, while identifying high-risk clusters through Bayesian spatial modeling. The BYM2 model revealed significant spatial heterogeneity in leprosy risk across the 645 municipalities, with relative risk estimates ranging from 0.06 to 31.52. Municipal wealth emerged as a significant protective factor (posterior mean: -0.059, 95% CrI: -0.081 to -0.037), indicating that economically advantaged areas consistently demonstrated lower leprosy incidence rates. The mixing parameter (φ = 0.517) suggested approximately equal contributions of structured spatial dependence and unstructured random variation in explaining disease distribution. Exceedance probability analysis identified distinct high-risk clusters primarily concentrated in western and northern regions of the state, where municipalities exhibited probabilities exceeding the threshold of RR greater than 2.0, representing areas with at least double the state average incidence rate.

The observed spatial clustering of leprosy cases reflects persistent socioeconomic disparities and suggests the influence of unmeasured environmental or social determinants operating at the municipal level. The concentration of high-risk areas in western and northern São Paulo aligns with historical patterns of regional development inequality, where these areas typically exhibit lower infrastructure investment and reduced access to specialized healthcare services. The stability of these spatial patterns over the four-year study period indicates sustained exposure conditions rather than temporary epidemiological fluctuations, similar to findings in other chronic infectious diseases where poverty-related factors create enduring transmission environments. The negative association between municipal wealth and leprosy incidence supports the well-established relationship between socioeconomic development and infectious disease burden, suggesting that comprehensive poverty reduction strategies may serve as effective primary prevention measures. Additionally, the substantial unexplained spatial variation captured by the random effects component indicates that factors beyond municipal wealth—such as housing quality, population density, healthcare accessibility, or cultural practices—likely contribute to disease transmission dynamics and warrant further epidemiological investigation.

This study demonstrates several methodological strengths, including the use of four years of comprehensive surveillance data from São Paulo's robust epidemiological system, ensuring high case ascertainment and diagnostic reliability. The BYM2 modeling approach effectively addressed the statistical challenges inherent in rare disease mapping by borrowing strength from neighboring municipalities and incorporating spatial dependence, thereby producing more stable risk estimates than traditional standardized incidence ratios. The integration of penalized complexity priors prevented overfitting while maintaining interpretability, and the exceedance probability framework provided a practical tool for public health priority setting. However, important limitations must be acknowledged. The use of municipal-level aggregated data may mask within-municipality heterogeneity and introduce ecological fallacy when inferring individual-level relationships. Residence at diagnosis served as a proxy for exposure location, potentially misclassifying individuals with complex migration histories or

long latency periods typical of leprosy. The model's limited covariate structure, while statistically significant, explained only a portion of the observed spatial variation, suggesting that crucial unmeasured factors—including individual-level sociodemographic characteristics, environmental exposures, and healthcare utilization patterns—remain unaccounted for. Furthermore, the high proportion of municipalities with low predictive accuracy (CPO < 0.01 in 98% of areas) indicates potential model misspecification or overdispersion that may affect the reliability of risk estimates in specific locations.

Conclusions

Leprosy distribution in São Paulo State exhibits significant spatial clustering associated with municipal wealth disparities. The persistent geographic patterns suggest sustained socioeconomic determinants affecting disease transmission. These findings support targeted public health interventions in identified high-risk areas and emphasize the importance of addressing structural inequalities in leprosy control strategies. Future research should explore approaches that integrate high-resolution spatial and temporal data with analyses stratified by vulnerable groups through spatio-temporal modeling frameworks to better understand disease dynamics and inform precision public health interventions.

References

Boigny, R. N., de Sousa Cavalcante, K. K., Florencio, C. M. G. D., Nogueira, P. S. F., Gomes, C. M., & Alencar, C. H. (2024). Temporal trends and space-time distribution of leprosy relapse in Brazil from 2001 to 2021. Transactions of the Royal Society of Tropical Medicine and Hygiene, 118(8), 537–549. https://doi.org/10.1093/trstmh/trae021.

Chen, W., Chen, Y., Cheng, Z., Chen, Y., Lv, C., Ma, L., Zhou, N., Qian, J., Liu, C., Li, M., Guo, X., & Zhu, Y. (2024). Global patterns of syphilis, gonococcal infection, typhoid fever, paratyphoid fever, diphtheria, pertussis, tetanus, and leprosy from 1990 to 2021: findings from the Global Burden of Disease Study 2021. Infectious Diseases of Poverty, 13(1), 66. https://doi.org/10.1186/s40249-024-01231-2.

Fundação SEADE. Índice Paulista de Responsabilidade Social – IPRS 2014-2018. São Paulo: SEADE; 2019. Available from: http://www.iprs.seade.gov.br/downloads/pdf/iprs_release_site.pdf.

Gelfand AE, Diggle PJ, Guttorp P, Fuentes M, editors. Handbook of Spatial Statistics. Boca Raton (FL): Chapman & Hall/CRC; 2010. ISBN: 978-1420072877.

Grijsen, M. L., Nguyen, T. H., Pinheiro, R. O., Singh, P., Lambert, S. M., Walker, S. L., & Geluk, A. (2024). Leprosy. Nature Reviews Disease Primers, 10(1), 90. https://doi.org/10.1038/s41572-024-00575-1.

Instituto Brasileiro de Geografia e Estatística (IBGE). Censo Demográfico 2022: Resultados Preliminares – População e Habitantes [Internet]. Rio de Janeiro: IBGE; 2023 [cited YEAR MONTH DAY]. Available from: https://www.ibge.gov.br/en/statistics/social/labor/22836-2022-census-3.html.

Lawson AB. Bayesian Disease Mapping: Hierarchical Modeling in Spatial Epidemiology. 2nd ed. Boca Raton (FL): Chapman & Hall/CRC; 2009. ISBN: 978-

1584888406.

Sczmanski, A. S., Pazin, L., Sakae, T. M., & Mazon, J. (2025). Analysis of the clinical and epidemiological profile of leprosy in Brazil and Major Regions. *Anais Brasileiros de Dermatologia, 100*(4), 501127. https://doi.org/10.1016/j.abd.2025.501127.

Simpson, D., Rue, H., Riebler, A., Martins, T. G., and Sørbye, S. H. (2017). Penalising model component complexity: A principled, practical approach to constructing priors. Statistical Science, 32:1–28.

Santacroce, L., Del Prete, R., Charitos, I. A., & Bottalico, L. (2021). *Mycobacterium leprae*: A historical study on the origins of leprosy and its social stigma. *Infezioni in Medicina*, *29*(4), 623-632. doi:10.53854/liim-2904-18.